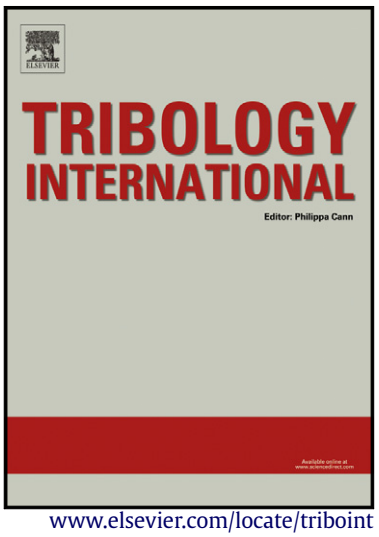

www.elsevier.com/locate/triboint

Ultrahigh vacuum system for advanced tribology studies: Design principles and applications

R.A. Nevshupa, M. Conte, A. Igartua, E. Roman, J.L. de Segovia

PII: S0301-679X(15)00030-4
DOI: http://dx.doi.org/10.1016/j.triboint.2015.01.020
Reference: JTRI3548

To appear in: *Tribology International*

Received date: 5 January 2015
Accepted date: 21 January 2015

Cite this article as: R.A. Nevshupa, M. Conte, A. Igartua, E. Roman, J.L. de Segovia, Ultrahigh vacuum system for advanced tribology studies: Design principles and applications, *Tribology International,* http://dx.doi.org/10.1016/j.triboint.2015.01.020

Ultrahigh vacuum system for advanced tribology studies: design principles and applications

R. A. Nevshupa[1], M. Conte[2,*], A. Igartua[2], E. Roman[3], J. L. de Segovia[3]
[1]IETCC-CSIC, C/Serrano Galvache 4, Madrid 28033, Spain

[2]IK4-Tekniker, Calle Inaki Goenaga 5, Eibar 20600, Spain

[3]ICMM-CSIC, C/Sor Juana Inés de la Cruz 3, Madrid 28049, Spain

Abstract
The main difficulty in designing of an ultrahigh vacuum (UHV) tribometer combined with tribophysical and tribochemical characterization techniques is to find the critical compromise between the scientific requirements and technical or technological limitations from different subsystems and components. The principal conflicts, their possible solutions and the recommended tribometer configurations are analysed. The developed methodological principles were applied for designing and construction of two UHV experimental tribological systems: TriDes-2 and Ca^{3}UHV. The advances in the design and development of the vacuum system as well as the UHV force sensor and sample holder are presented and discussed.

Keywords: UHV tribometer; force sensor; gas desorption.

1. Introduction
In the 1960s, the space exploration needs prompted an increased research on problems related with friction, wear and lubrication in vacuum and controlled atmospheres [1]. That research was focused on the accelerated life testing of the mechanisms and components, as well as on developing and testing new lubricants and protective coatings. For this purpose a number of vacuum test equipment were developed covering a gas pressure range from low to ultrahigh vacuum [2]. By the early 1970's, when some of the problems had been resolved and the limitations of other had been defined, most of the research stopped.

However, recently tribological systems again have become the limiting factor in spacecraft reliability and performance since a number of new applications have arisen stimulating a renewed interest [1-3]. Advanced tribological materials should also comply with very strict requirements on the outgassing of volatiles [4] as well as on secondary electron emission both from free surfaces and during friction and mechanical deformation [5, 6] in order to avoid contamination of lenses, sensors and other devices to prevent the multipactor effect. Therefore, vacuum test equipment should allow to study those phenomena. Similar problem exists in the modern semiconductor industry: the need to enhance yield of the semiconductor chips with ever-smaller elements challenges the engineers of manufacturing systems to reduce number of

* Now at: Anton Paar TriTec SA, Rue de la Gare 4, 2034 Peseux, Switzerland; and Empa, Laboratory of Mechanics of Materials and Microstructures, Feuerwerkerstrasse 39, 3602 Thun, Switzerland

chip defects associated with gaseous and particulate contamination that in large part originates from mechanical elements [7, 8].

On the other hand, there is a steadily growing interest in basic studies on the fundamental mechanisms of friction, wear, lubrication and related tribophysical processes and tribochemical reactions. Ultrahigh vacuum and/or controlled ambient atmosphere are the necessary conditions when studying gas-phase lubrication [9], mechanically stimulated gas emission (MSGE) [10-20], triboplasma [21-23], triboelectrification [24-26], triboluminescence [24, 27, 28], emission of charged particles [29-31], tribochemical reactions [23, 32-34], etc. For these studies, conventional tribological test rigs should be combined with various physical, chemical and surface characterization techniques.

So far, various vacuum test equipment has been developed to address the needs of specific tribological characterization of materials in vacuum and under controlled atmosphere [2, 15, 30, 35-46]. Some of these systems have optimal design, although "trial and error" has been the general approach. Development of a test equipment with controlled vacuum or gas environment aimed to answer to various scientific, technical and technological challenges associated with the tribological problems is not a trivial task since many, and often conflicting, requirements must be met. Lack of a methodological basis complicates the optimal development of vacuum test equipment making this task more art than science.

Bearing in mind that a vacuum tribometer for low vacuum can be developed by just placing a conventional tribometer inside a corresponding vacuum chamber the present work is focused on the designing of high and ultrahigh vacuum systems. We endeavour to suggest the ways of optimal designing of vacuum tribological test rigs finding a compromise between the requirements and limitations. This analysis was used by the authors for the development of two novel experimental systems in which tribological and tribo-physico-chemical characterization of materials and lubricants can be carried out. The authors believe that the developed approaches and lessons learnt in this work will underpin further development of these techniques.

2. Basic principles of design

2.1. General requirements and challenges

While tribological characterization is aimed at determining friction and wear properties of the materials under various experimental conditions and environment, tribo-physico-chemical (TPC) studies involve characterization of physical and chemical phenomena activated at the tribological contact. These phenomena can be studied using specific experimental techniques coupled to a conventional tribometer. As a result, an experimental system is much more sophisticated than just a vacuum tribometer that is quite complex per se.

Generally, an experimental system for combined tribological and physico-chemical characterization comprises the following seven subsystems: vacuum system, mechanical system, sensors, sample handling and manipulation, environment control, control of loading and kinematics, techniques for physico-chemical (TPC) characterization. Optimal designing of the experimental system implies finding a satisfactory compromise between the requirements set by these seven subsystems upon the environmental and operational conditions, relative position of the components and their compatibility, which problem can be called "Septilemma". The schematic drawing of the subsystems and relations between them is shown in Fig. 1. Detail analysis of all relationships and conditions set by each of the subsystems is out of the scope of

this work and can be consulted elsewhere [47]. Some relevant specific problems between the subsystems are discussed below.

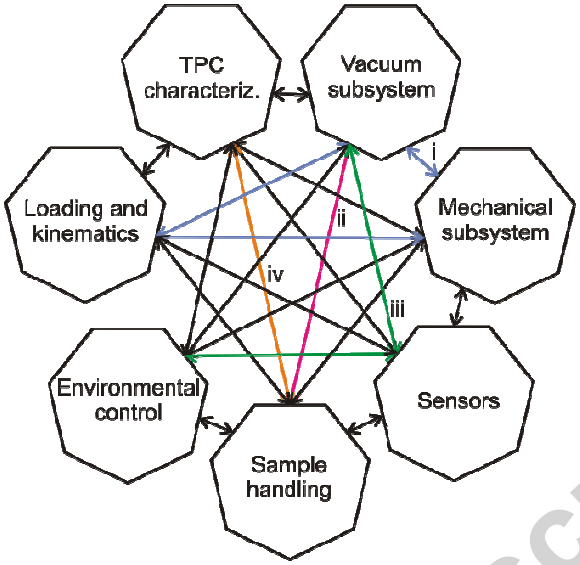

Figure 1. Subsystems of a vacuum test rig for complex tribological and tribo-physico-chemical (TPC) characterization of materials. Some of the critical relationships and constrictions between the subsystems are shown by arrows: i (blue) – limitations between Vacuum, Mechanical and Loading and Kinematics subsystems; ii (red) – limitations between Vacuum and Sample handling subsystems; iii (green) – limitations between Sensors, Environmental control and Vacuum subsystems; iv (orange) – limitations between Sample handling and TPC subsystems.

Vacuum system against mechanical, loading and kinematics subsystems (links i in Fig. 1). Optimal mechanical design of a system implies the right selection of constructional materials. The mechanical structure must have sufficiently high stiffness in order to increase the eigenfrequency and reduce the effect of low frequency oscillations on the stability of loading, relative position of the pin and the sample, motion and friction force measurements. The Mechanical system has to ensure also the required level of the vibroinsulation from the basement and from mechanical and turbomolecular pumps. Furthermore, these materials must fulfil the requirements of an ultrahigh vacuum system such as low outgassing rate, low adsorption capacity, resistance to outgassing baking temperature in the range between 100 ºC and 400 ºC. The effectiveness of the pumping out has to be considered: blind tapped openings should be avoided, internal cavities must be connected with the vacuum chamber or the pumping line by the ducts of sufficient conductance for rapid evacuation of the gases, the configuration of the internal elements should be optimized in order to reduce nonuniformity of pressure due to dynamic processes, etc. When very high stability of gas pressure is required, such as for the measuring of MSGE, pressure variation due to contraction and expansion of the bellows in the loading and kinematics subsystems must be taken into account.

Vacuum system against sample handling (link ii in Fig. 1). For high and ultrahigh vacuum systems the time required to achieve gas pressure below 10^{-7} hPa after venting can be significantly reduced by using a load-lock system (LLS). However, sample handling in a system with LLS is much more complicated and requires using of special long-travel manipulators with various degrees of freedom, devices for locking and unlocking the sample holder, etc.

Furthermore, the components of the sample handling system must meet the requirements and limitations of the environmental control subsystem (sample temperature control) and TPC characterization (bias electric potential, tribocurrent, etc.). The sample holder must fulfil at least the following requirements: good thermal contact with the base surface (for the sample heating and cooling), good wear resistance and low friction (to make easier sample manipulation), be insulated from the ground and should be electrically biased (for tribocurrent, tribopotential and triboemission characterization). Also, it can be necessary to plug in to the sample holder a temperature sensor using a special connector suitable for vacuum. Higher and lower temperatures of the sample require special setups in order to cut off the undesired infrared emission from the environment to a cold sample or from the hot sample to the environment. Cooling to cryogenic temperatures may require also special measures to reduce vibrations produced by the cooler and cooling agent flows.

Sensor against vacuum and TPC subsystems. The force sensors are used to measure and control the normal and friction forces. An additional displacement sensor can be used for indentation. All the sensors must be vacuum-compatible with low desorption rate and suitable for moderate outgassing baking temperature. Furthermore, the force and displacement sensors must not interfere with TPC devices. For example, strain gauges, capacitive and inductive displacement sensors can produce electromagnetic interference on charge detectors, electron multipliers, antennas and other sensitive devices. Therefore, optical sensors can be a good alternative for other displacement sensors. However, optical sensor can be a problem for measuring triboluminescence.

Optimal solution of the septilemma can be found using multi-objective or Pareto optimization method [47]. This method consists in step-wise optimization of the design parameters considering sequentially each specific objective and associated set of constrictions and limitations. In case, the design parameters and the specific objectives are discrete values, the optimal solution can be found by searching the most adequate options from the list of parameters. When the design parameters and specific objectives are continuous variables, finding the optimal solution is not an easy task, which can be solved using the method of mathematical programming (for details see specific literature, e.g. [48]).

2.2. Tribometer configurations

This work is focused on the systems for the macro- to micro-newton range. Some of the conclusions drawn in this work are applicable to a nano-newton range system, however as the latter is quite different in design, it is not considered in this work. The majority of UHV tribometers use a reciprocating motion since this configuration allows to keep all the mechanical bearings and guides outside a vacuum system and transmit the motion into the chamber using a shaft connected to the actuator, which can be sealed with all-metal flexible bellows without use of non-metal gaskets.

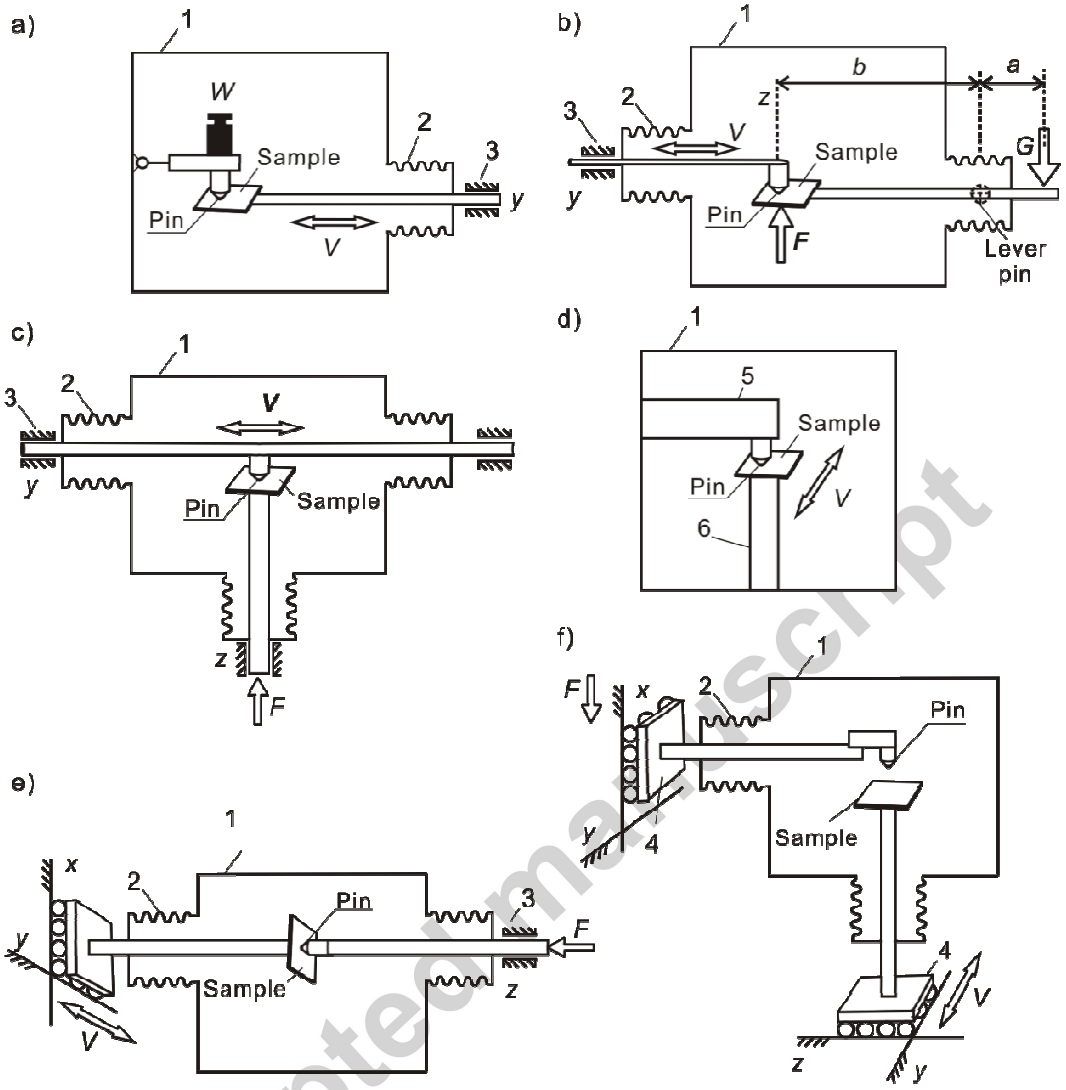

Figure 2. Schematic drawings of some configurations of reciprocating motion vacuum tribometers: a) a system with a dead load applied inside a vacuum chamber; b) a system with a lever system to apply a dead load from the atmospheric side; c) a system with symmetrical support of the pin; d) a system with the drives situated in vacuum; e) a system with 3 degrees of freedom and opposite pin and samples shafts; f) a system with 4 degrees of freedom and with the sample and pin shafts at 90º position. 1 – a vacuum chamber; 2 – bellows; 3 – bearings or guides for the shafts; 4 – two-axes ball guide; 5, 6 – vacuum drives (piezo drives, etc.)

Figure 2 shows schematic drawings of several reciprocating motion vacuum tribometers some of which has already been constructed. The simplest configuration is shown in Fig 2 a) in which the sample connected to the shaft performs reciprocating linear motion while the normal load is applied to the indenter by the dead load *W*. The evident shortcoming of this configuration is that the normal load cannot be continuously changed from the outside. The scheme b) uses a lever, that one arm is connected to the bearings situated at the outer atmosphere while another arm is in vacuum. The bearings and flexible bellows allow tilting the lever with negligible resistance torque. Thus, when a load *G* is applied to the atmospheric arm of the lever, it produces the reaction *F* between the sample at the end of the vacuum arm and the indenter (the pin). The pin is connected to a sealed shaft and can perform reciprocating linear motion. This scheme was

realized in an UHV experimental system TriDes [49]. In this configuration, when the lever and the shaft axes are parallel, normal load can slightly vary (various percent) during a friction cycle because of the variation in the effective arm length. This shortcoming can be overcome by placing the shaft at 90º to the lever. Furthermore, the maximal allowable normal load can be increased by using two bearings symmetrically on both sides of the chamber (Fig. 2 c) [45].

Recent advances in the development of polymeric materials and actuators suitable for operation in UHV, e.g. piezo flexure actuators, piezo motors, etc., provide the possibility to place the whole drive inside a vacuum chamber, thus making the design more compact due to elimination of auxiliary elements such as flexible bellows and reduction of the inertia and power consumption (Fig. 2 d). Though having limited load capacity, these drives are promising for the use in UHV tribometers. Nevertheless, in combination with sensitive electric sensors piezo drives must be used with caution since they can produce electromagnetic interferences.

The systems with 3, 4 and more degrees of motion (Fig. 2 e and f) have the advantage of flexibility in selection different zones on the sample for the test. In these systems, like in the system Ca^{3}UHV, unidirectional sliding can also be done on open and close trajectories by using a proper motion control of the *x*-*y* stage. In some systems the indenter has an additional rotational degree of freedom with respect to *z* allowing changing the contacting zone on the pin between the tests without changing the pin [35, 50].

Concerning rotary motion, it can be realized in two ways: using either bearing inside vacuum or some kind of a seal for the rotating shaft. Sliding seal is usually inacceptable in UHV because of high gas leak rate. Therefore, a range of all-metal rotary-motion drives with and without reduction which can sustain outgassing baking has been developed for different specific requirements [47]: high load, increased position accuracy, etc. However, these drives have large number of various tribological contacts including rolling bearings, harmonic gears, planetary gears, etc. that results in increased outgassing due to MSGE [7]. Recently, advanced seals, e.g., with magnetic fluid, that can provide required leaking rate below 10^{-11} hPa l s^{-1} have appeared. These seals can be used in a certain range of sliding velocity and mechanical tolerances of the shaft, but they can be undesirable for TPC characterization due to possible chemical reactions between the components of the sealing liquid with the emission products.

From the tribological point of view, it does not matter which part, the indenter or the sample, moves in the test. However, for TCP characterization the scheme in which the indenter is still preferable, since the analytic equipment such as microscope, laser, electron and ion detectors, etc. can be easier focused on the stationary contact zone.

3. Development of advanced UHV tribometers and lessons learnt

The methodology briefly described in the previous section was used by the authors to construct two UHV systems, named TriDes-2 and Ca^{3}UHV, for tribological, mechanical and tribochemical characterizations of solid materials, coatings and lubricants under residual vacuum and in controlled gas environment. TriDes-2 was specially designed for the characterization of MSGE, tribochemical and tribophysical processes, while Ca^{3}UHV is a universal reciprocating motion tribometer that also can be used for the characterization of triboemision of gases and other TPC processes. The general characteristics of the systems are listed on Table 1.

Table 1. General characteristics of the systems TriDes-2 and Ca^{3}UHV

Parameters	TriDes-2	Ca^3UHV
Range of the normal load (N)	0.1-8	0.1-20
Range of the sliding speed (mm s^{-1})	0.1-5	0.002-10
Maximal displacement of the pin (mm)	7	20
Sample temperature (ºC)	Ambient	Cryogenic – 350 [1)]
Gas pressure range (hPa)	10^{-5} – 10^{-10}	10^{3} – 5×10^{-9}
Maximal allowable gas pressure variation during the test (% /min)	2.5×10^{-3}	2.5×10^{-3}
Volume of vacuum chamber (l)	4	9.6
Pumping line conductivity (l s^{-1}, for N_2):		
main line	3.59±0.14	183±9
diaphragm	3.82±0.15	7.4±0.4
Time constant of pumping process for N_2 (s): main line / through the diaphragm / main line+ diaphragm	1.11/ 1.05/0.55	0.052/1.3/0.05
Types of the tests	Reciprocating linear sliding, indentation, scratch [2)]	Reciprocating linear sliding

[1)] Optionally up to 500 ºC

[2)] Optionally

Below, some of the lessons learnt in the development of these two systems are discussed.

3.1. Design of a vacuum system and environment control

The system TriDes-2 was designed to operate under high vacuum (HV) and UHV (5 orders of magnitude of pressure), while the pressure range of Ca^3UHV covers 13 orders of magnitude (Table 1) that leads to much more complex design. The strictest requirements are associated with UHV range, where all materials and components must have very low specific rate of gas and volatile emission and be able to sustain repetitive cycles of outgassing baking. When an UHV system is operating under low and medium vacuum (LV), i.e. in the pressure range 10^{3}–10^{-3} hPa, one should bear in mind the potential risk of surface contamination, which can lead to time-consuming and costly cleaning and degassing treatment. This is the price for the extended gas pressure range, which however, is justified, when the tests under LV are seldom. In this case the investment in a universal system is smaller than in two tribometers for high and low vacuum separately.

To obtain vacuum in both systems there is a combination of a turbomolecular pump (TMP) *2* and a forepump *3* with the lowest attainable pressure around 10^{-10} hPa (Fig. 3). Additional UHV pumps (ion, cryogenic, etc.) can be installed to achieve even lower gas pressure. To introduce the gases and control the gas pressure there is an automatic leak valve *9* with a maximum conductance of 0.7 l s^{-1} (for N_2) and the range of gas flow 10^{-10} – 600 hPa l s^{-1} which can operate in parallel with a TMP. In order to achieve the gas pressure slightly higher than 10^{-6} hPa it is necessary to control the gas load of the TMP using a butterfly valve *12*. Finally, at even higher gas pressures (>10^{-4}) the TMP must be off and the required pressure can be achieved by varying the leak rate when pumping by a forepump. In this case the adequate precautions must be taken to avoid contamination of the chamber by backflow of oil vapours from the forepump.

For accurate quantification of MSGE rate under HV and UHV a dynamic gas expansion method is used in both systems. For this purpose the main chamber *1* is pumped through a diaphragm *7* with well-defined gas conductance, while the main valve *4* is closed. The gas emission rate is proportional to the difference in the pressure increase on the sides of the diaphragm, which is

measured using the calibrated gauges *5* and *8*. The details of the method are described elsewhere [13, 51, 52].

When during the test the sample must be kept chill or hot, the gas emission from the heater and gas adsorption on a cryogenic cooler may alter the base pressure and affect the MSGE measurement. To face this problem a special sample holder *14* has been designed and patented [53]. The sample holder *1* (Fig. 4) has a supplementary small vacuum chamber *4* situating inside the main vacuum chamber and surrounding the heater and/or the cooler. This chamber is formed by a shield *2*, which separates vacuum volume in two independent parts. The shield is maintained at the same temperature as the main chamber. The supplementary chamber *4* is pumped by a separate pump or by the main pump through the line *15*. Since thermal conductivity and convection in vacuum are negligible, the shield cut the thermal radiation from the heater to the main chamber and from the main chamber to the cooler. Sealing of the supplementary chamber *4* can be done in one of the two ways: either by using an element *3* with very low thermal conductivity and gas emission rate, such as thin stainless steel foil welded to both the shield and the sample holder, or by a labyrinth sealing *5* in which thermal isolation between *2* and *1* is achieved by thin vacuum gap, whereas the gas flow from/to the supplementary chamber *4* is largely limited due to the zigzagging geometry. Experimental measurements of a conductivity of the labyrinth seal of Ca^{3}UHV yielded value of only 0.439±0.005 l s^{-1} (for N_2) that is small enough to largely cut off the gas flows from the heater as well as towards the cooler of the sample holder and maintain stable the base pressure.

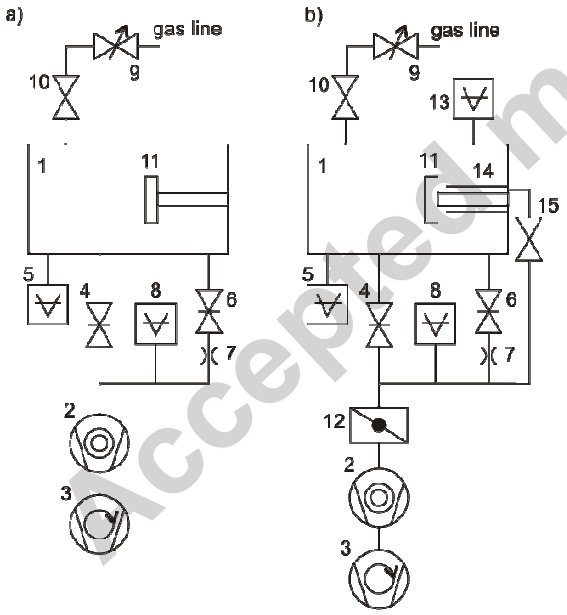

Figure 3. Schematic drawing of main vacuum systems: a) TriDes-2; b) Ca^{3}UHV.

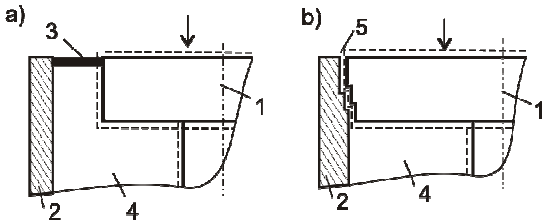

Figure 4. Two schemes of sealing the supplementary vacuum chamber of the sample holder: a) with material of low thermal conductivity; b) using labyrinth seal. 1 – the sample holder with a heater and/or chiller; 2 – the screen; 3 – gasket of low thermal conductivity; 4 – supplementary vacuum chamber of the sample holder; 5 – labyrinth seal; hot/chill surface is shown by the dashed line. The surface where the sample to be placed is shown by the arrow.

When measuring transitory gas pressure during reciprocating motion, the dynamic limitations of the vacuum system should be consider. In terms of signal processing, a vacuum system is defined as an integral function, so the time series of pressure are smoother than corresponding gas desorption rate. In order to resolve pressure peaks the vacuum system must have a time constant below 20% of the characteristic time of the vacuum process. This can be achieved by reducing the volume of the chamber and increasing the pumping speed. However, the pumping speed has to be as low as possible for accurate measuring of the desorption rate. Therefore, it is desirable to have in the tribometer the means for variation of the pumping speed in order to find the optimal balance between the sensitivity of gas emission measurement and resolution of peaks in pressure time series in each particular experiment. For this purpose in both TriDes-2 and Ca^{3}UHV the experimental chamber can be pumped through one of two pumping lines with high and low conductivities which values are listed in Table 1. In addition, Ca^{3}UHV has a butterfly valve which can be used for reducing the pumping speed of the TMP.

Figure 5 illustrates the effect of the pumping speed on gas pressure time series resulting from MSGE. Both time series were obtained using TriDes-2 before and in the course of rubbing of Armco iron sheet by an alumina ball, 2 mm in diameter, under the same experimental conditions (normal load 0.73 N, sliding speed 0.18 m s^{-1}, frequency of reciprocating motion 10 back and forth strokes per minute) with the exception of the pumping speed (for N_2) that was 7.41±0.41 and 3.82±0.15 l/s, for graphs i and ii, correspondingly. With no rubbing the gas pressure, p_{base}, in the chamber was steady in each case, although for ii it was almost two-fold higher than for i. This is reasonable since, for the same rate of gas emission from the walls of the chamber, the base pressure is inversely proportional to the pumping speed. When rubbing started, the gas pressure sharply rose due to MSGE from iron. Again, in case ii, the maximum pressure increase, Δp_{max}, was higher than in case i. Furthermore, signal-to-noise ratio was better in case ii due to increase in signal intensity while the noise dispersion was the same in both experiments.

Double peaks of gas pressure corresponding to forth and back sweeps of the indenter can be distinguished in the graphs. Note that the time interval between the back and forth sweeps in one cycle was shorter than between the cycles [51]. Though the amplitudes of these peaks, Δp_{peak}, were almost the same in both cases, their relative intensity, i.e. the ratio Δp_{peak} / Δp_{mean}, were quite different: 0.0563±0.0051 and 0.0331±0.0018 for i and ii, correspondingly. The higher is the relative intensity of the peaks, the higher is the resolution. This difference can be seen better in the inset of Fig. 5 where both graphs, normalized to (0;1), are plotted on the same axes. Another important parameter that has to be considered when studying transitional processes of MSGE is the rate of pressure decay. Higher rate of pressure decay that is associated with higher pumping speed results in less distortion and more accurate definition of features of pressure time series. However, in this example, the influence of the pumping speed was insignificant since the time constants of pumping process (0.55 and 1.05 s for i and ii, correspondingly) were more than five-fold smaller than the time constant of gas emission decay (36.1 s). These results suggest that increase of the pumping speed leads to enhancement of the peak resolution and decrease of distortion of pressure time series at the expense of decrease in both sensitivity and signal-to-noise ratio.

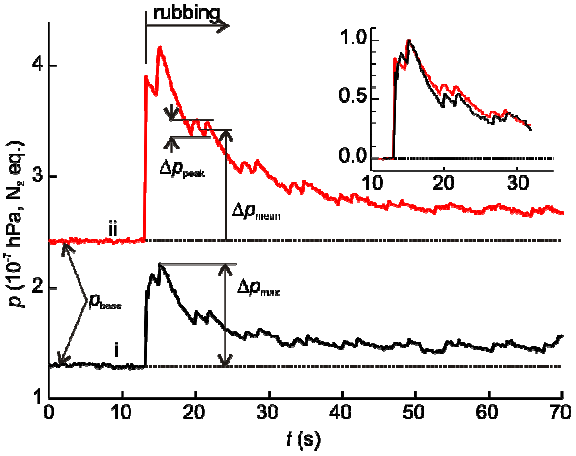

Figure 5. Gas pressure time series due to MSGE from Armco iron sheet under reciprocating rubbing by an alumina ball. The experimental conditions were the same with the exception of the pumping speed that was 7.41±0.41 and 3.82±0.15 l/s for i and ii, correspondingly. Inset shows the graphs normalized to (0;1).

3.2. Force sensors

Force sensors being the most important and critical elements for accurate tribological measurements have to respond to some important criteria, like vacuum compatibility, accuracy and repeatability. Even though the preferable way of measuring a force is the direct one, in the most of vacuum tribometers the indirect sensors are used due to geometrical and constructive reasons. Indirect method consists in the deflection measurement of a spring with well-defined spring constant and good linearity by means of strain gauges, capacitive, optical or inductive sensors, etc. As it has been already discussed in Section 2, optical sensors are preferable when TPC processes have to be characterized. For the indirect force measurement it is necessary to bear in mind the effect of misalignment of the spring. If only one flexible member is used (Fig. 6 a), tilting of a mirror can produce a consistent error; if more than one flexible member is used in parallel mounting, the total displacement remain parallel but a warpage effect can occur due to additional torque when a tangential force is applied to the tip at a distance l_w from the longitudinal axis of the double-leaf spring (Fig. 6 b).

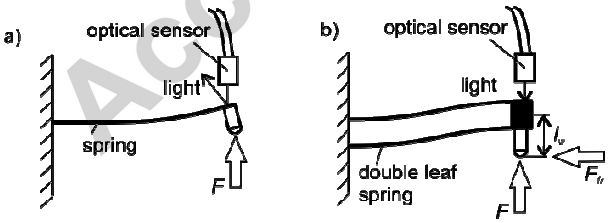

Figure 6. Schematic drawing of a force sensor with a single leaf spring (a) and double-leaf spring (b)

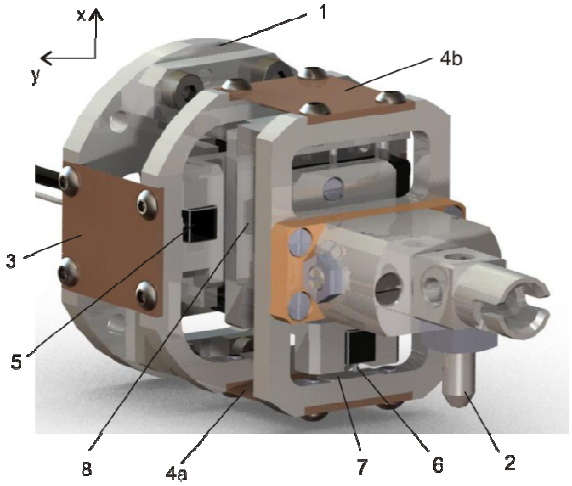

Figure 7. UHV compatible 2-axes force sensor. 1 – the base plate; 2 – the pin; 3 – one of two leaf springs used for measuring *y* component of the force; 4a and 4b – the leaf springs for measuring *x* component of the force; 5, 6 – bundle optical fibre displacement sensors; 7 – mirror of the *x*-stage; 8 – microactuator for positioning of the optical sensor of the *y*-stage.

In both TriDes-2 and Ca^{3}UHV, intensity modulation bundle fibre optic sensors are used. These sensors require pre-setting the correct distance between the sensor and the mirror attached to a spring before each measurement. In addition, an intensity calibration must be carried out regularly by scanning the distance between the mirror and the sensor, while measuring the output time series. These manipulations can be done in atmosphere during venting the system by using manually operated external micropositioners [54]; however, obtaining the required vacuum after each adjustment of the sensor is time consuming and costly. Furthermore, small structural deformations of the system due to the pressure difference and thermal deformations induced by outgassing baking may cause misalignment of the sensors and the need of new adjustment. Therefore, in Ca^{3}UHV system these problems were overtaken using vacuum-compatible built-in linear-motion microactuators which allow relative displacement (up to 5 mm) of the sensor against the mirror (Fig. 7). Another advantage of this patented [55] solution is that it allows selecting the sensitivity of the measuring between the tests without venting the system by situating the sensor in its near or far measuring ranges. This leads to increase of the range of the force measuring about one order of magnitude. For details on the operation principle of the sensor see [56].

Recent analysis revealed the critical importance of the quality of the reflecting surface on the measurement uncertainty of the intensity-modulation bundle fibre-optic displacement sensors [56]. Presence of several defects may significantly increase the uncertainty of the measurement, especially for *x*-stage, which sensor can be displaced in both *x* and *y* directions with respect to the mirror. Therefore, the mirror should be preferably a polished hard metal, e.g., hardened stainless steel, rather than a thin film. In addition, in order to increase the durability of the mirror and reduce the risk of its damage by the sensor during the operations of the pin exchange, the optical sensor can be moved away from the mirror using the linear micro actuator.

3.3. Motion system

Though there are several commercially available solutions for integrating a 3-axes motion system inside a high vacuum chamber, everything becomes more complex when we switch to UHV, mainly due to requirements on outgassing and baking cycles. In many cases, an indirect

driving of the parts is needed, that is a mechanical transformation of the motor output power using belts, screws, gears, etc. It leads to an increase in the dead volumes and outgassing surfaces as bellows must be used. Regarding the latter, it should be kept in mind that a proper baking for reaching UHV should include all these supplementary surfaces; therefore, the complexity of the system increases significantly.

Another problem is related to the increased mass and inertia of the motion stages due to the use of additional sealing elements. On the one hand, this leads to reduced rigidity and limits the maximal allowable forces. On the other hand, it restrains both the maximal achievable acceleration and velocity. In fact, the maximal achievable acceleration depends on the stalled-motor current, I_{st}, which is proportional to the force, F_{st}, needed to start motion:

$$I_{st} \propto F_{st} = ma + F_{fr}, \quad (1)$$

where m is the mass of the moving components, a is the acceleration and F_{fr} is the static friction force. For the sake of simplicity we can consider that magnitudes of acceleration and deceleration are the same. Then, with the maximum displacement, L, limited due to geometrical restrictions of vacuum sealing elements, the maximal achievable velocity, V_{max}, is given by:

$$V_{max} = \sqrt{aL} = 0.5aT, \quad (2)$$

where T is the duration of a motion cycle (Fig. 8). As can be seen from the plot, when desired velocity, V^*, approaches V_{max}, the acceleration and deceleration intervals, t_a and t_d, correspondingly, become considerably large, while the time interval, t_v, when the velocity is constant shortens. So, mean sliding velocity increases slower than V^*:

$$V_{mean} = V^*\left(1 - \frac{V^*}{2\sqrt{aL}}\right). \quad (3)$$

The acceleration can be increased by selecting a motor with higher power and stalled current, but it also leads to undesirable vibrations at the inversion of the motion and is costly. Another way consists in optimization of the design by reducing the size and the mass of the motion system as well as by using different actuators, e.g., long-travel and high carrying capability piezoactuators or advanced hydraulic actuators with magnetic fluid [57].

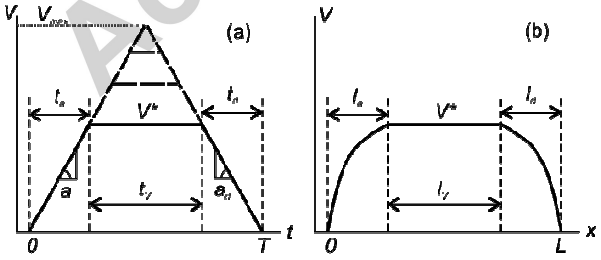

Figure 8. Diagram of velocity in a sliding cycle: a) as function of time; b) as function of sliding distance.

In Ca^{3}UHV system having the configuration f (Fig. 2) and intended to study very low MSGE rates induction (synchronous) servomotors were chosen for motorization of the axes x, y and z. This kind of motor has the advantage of no need of mechanical commutation since the electric

current in the rotor is obtained by electromagnetic induction from the magnetic field of the stator winding. Also these motors have low inertia, high velocity, no slip and low maintenance. The motors equipped with absolute encoders are controlled by the corresponding drivers connected to the motion control through a SERCOs bus. The maximal acceleration obtained was 20 mm s^{-2}. In TriDes-2 system two stepper motors with microstep option have been used for loading and auxiliary displacement of the sample in the direction perpendicular to the sliding one, while a synchronous motor has been used for reciprocating sliding motion. Without special driver step motor should not be used for sliding motion because of intrinsic instability of the sliding speed, especially at slow motion.

4. Conclusions

Designing of an UHV tribometer system is a much more complex task than for a tribometer working at atmosphere since a number of contradictory requirements and limitations must be met. This task can be simplified by a correct classification of the parameters, requirements and limitations according to seven main subsystems of the UHV tribometer. Then, step-wise optimization of the design parameters can be carried out considering sequentially each specific objective and associated set of constrictions and limitations.

Though advanced seals have been developed recently for rotating shafts, the linear reciprocating motion configuration remains preferable for the UHV tribometers intended for studying of various tribochemical and tribophysical process. Combination of the tribometer with physical and chemical experimental techniques set strict requirements on the subsystems of the tribometer in terms of: stability of the base pressure, compatibility of the materials and components of all subsystems, electric isolation of the pin and the sample from the ground, etc. Some of the advantages from the development of two UHV tribometer systems are presented and discussed. A vacuum system was developed to control the environment in the pressure range from 5×10^{-9} hPa to atmospheric. In order to reduce the instability of the base pressure related to gas adsorption on the cooler and desorption from the heater of a sample holder, a special design with a labyrinth seal or a special gasket of low thermal conductivity has been developed and patented. Also, a two-stage force sensor based on the intensity-modulated bundled optical fibre displacement gauge was developed. The novelty of this sensor consists in the use of linear motion micro actuators for adjustment of the relative position of the optical sensor in situ. This design allows extending the range of measured forces about one order of magnitude due to utilization of both measuring ranges of the optical sensor. The need of using sealing bellows increases the mass and reduces the rigidity of the motion system. Therefore, the maximum allowable load as well as the maximum achievable sliding speed are usually smaller for the UHV tribometer in comparison with a tribometer working at atmosphere. The acceleration and deceleration intervals cannot be ignored in many cases and significantly reduce the mean velocity.

Acknowledgements

The authors thank K. Cruz, A. Delgado, K. Garmendia and E. Berriozabal for technical assistance. This work was financially supported by the Spanish Ministry of Economy and Competitiveness with the participation of the European Regional Development Fund (FEDER) of the European Union under the projects CIT-420000-2009-53, RYC-2009-0412, BIA2011-25653 and IPT-2012-1167-120000. Also the authors acknowledge the support from the Government of Basque Country through the program EMAITEK.

References

[1] Miyoshi K. Solid Lubricants and Coatings for Extreme Environments: State-of-the-Art Survey. TECHNICAL MEMORANDUM. Cleveland, Ohio: National Aeronautics and Space Administration, Glenn Research Center; 2007. p. 16.
[2] Jones WR, Jansen MJ. Space tribology. Hanover, MD: NASA Center for Aerospace Information; 2000. p. 33.
[3] Colas G, Saulot A, Bouscharain N, Godeau C, Michel Y, Berthier Y. How far does contamination help dry lubrication efficiency? Tribology International 2013;65:177-89.
[4] ESA E. Space product assurance. Thermal vacuum outgassing test for the screening of space materials. Noordwijk: ECSS Secretariat, ESA-ESTEC; 2008. p. 45.
[5] Fischer D. Untersuchung von Reibungsvorschungen mit Hlfe der Exoelektronenemission. Berlin: Berlin Technical University; 1970.
[6] Buckley DH. Friction, Wear, and Lubrication in Vacuum: Scientific and Technical Information Office, National Aeronautics and Space Administration [available from National Technical Information Service, Springfield, Va.]; 1971.
[7] Nevshupa RA, Roman E, de Segovia JL. Contamination of vacuum environment due to gas emission stimulated by friction. Tribology International 2013;59:23-9.
[8] The international technology roadmap for semiconductors. Yield enhancement. ITRS; 2009.
[9] Martin J-M, Bouchet M-IDB, Matta C, Zhang Q, Goddard WA, Okuda S, et al. Gas-Phase Lubrication of ta-C by Glycerol and Hydrogen Peroxide. Experimental and Computer Modeling. The Journal of Physical Chemistry C 2010;114:5003-11.
[10] Řepa P. Mechanically induced desorption. Vacuum 1992;43:367-71.
[11] Nevshupa RA, de Segovia JL. Outgassing from stainless steel under impact in UHV. Vacuum 2002;64:425-30.
[12] Peressadko AG, Nevshupa RA, Deulin EA. Mechanically stimulated outgassing from ball bearings in vacuum. Vacuum 2002;64:451-6.
[13] Nevshupa RA, de Segovia JL, Roman E. Surface-induced reactions of absorbed hydrogen under mutual mechanical forces. Vacuum 2005;80:241-6.
[14] Buckley DH, Johnson RL. Friction, wear and decomposition mechanisms for various polymer compositions in vacuum to 10^{-9} millimeter of mercury. Washington D.C.: NASA; 1963. p. 28.
[15] Kragelskii IV, Lubarsky EM. Friction and Wear in Vacuum. Moscow: Mashinostroenie; 1973.
[16] Wilkens W, Kranz O. The formation of gases due to the sliding friction of teflon on steel in ultrahigh vacuum. Wear 1970;15:215-27.
[17] Frisch B, Thiele W-r. The tribologically induced effect of hydrogen effusion and penetration in steels. Wear 1984;95:213-27.
[18] Ishikawa Y, Yoshimura T. Mechanically stimulated outgassing from stainless steel surface. Journal of Vacuum Science & Technology A: Vacuum, Surfaces, and Films 1991;9:2021-4.
[19] Amelin AV, Muinov TM, Pozdnyakov OF, Regel VR. Comparison of the mass spectra of the volatile products liberated from polymers in the course of mechanical destruction and thermal degradation. Mechanics of Composite Materials 1967;3:54-60.
[20] Nevchoupa RA, de Segovia J, Deulin EA. An UHV system to study gassing and outgassing of metals under friction. Vacuum 1999;52:73-81.
[21] Miura T, Nakayama K. Two-dimensional spatial distribution of electric-discharge plasma around a frictional interface between dielectric surfaces. Applied Physics Letters 2001;78:2979-81.
[22] Nakayama K, Nevshupa RA. Plasma generation in a gap around a sliding contact. J Phys D Appl Phys 2002;35:L53-L6.
[23] Heinike G. Tribochemistry. Munchen: Carl Hanser Verlag; 1984.

[24] Nevshupa RA. Effect of gas pressure on the triboluminescence and contact electrification under mutual sliding of insulating materials. Journal of Physics D: Applied Physics 2013;46:185501.
[25] Hiratsuka Ki, Hosotani K. Effects of friction type and humidity on triboelectrification and triboluminescence among eight kinds of polymers. Tribology International 2012;55:87-99.
[26] Williams MW. Triboelectric charging of insulating polymers-some new perspectives. AIP Adv 2012;2.
[27] Walton AJ. Triboluminescence. Advances in Physics 1977;26:887-948.
[28] Nevshupa RA, Nakayama K. Triboemission behavior of photons at dielectric/dielectric sliding: Time dependence nature at 10^{-4}-10^{4} s. J Appl Phys 2003;93:9321-8.
[29] Nakayama K, Ikeda H. Triboemission characteristics of electrons during wear of amorphous carbon and hydrogenated amorphous carbon films in a dry air atmosphere. Wear 1996;198:71-6.
[30] Nevshupa RA, Nakayama K. Effect of nanometer thin metal film on triboemission of negatively charged particles from dielectric solids. Vacuum 2002;67:485-90.
[31] Evdokimov VD. Specific features of exoelectron emission during friction of metals. Soviet Physics Journal 1968;11:11-3.
[32] Le Mogne T, Martin J-M, Grossiord C. Imaging the Chemistry of Transfer Film in AES/XPS Analytical UHV Tribotester. In: Dowson D, editor. Lubrication at the Frontier: The Role of the Interface and Surface Layers in the Thin Film and Boundary Regime. Amsterdam: Elsevier; 1999. p. 413-22.
[33] Dante RC, Kajdas CK. A review and a fundamental theory of silicon nitride tribochemistry. Wear 2012;288:27-38.
[34] Kajdas CK. Importance of the triboemission process for tribochemical reaction. Tribology International 2005;38:337-53.
[35] Martin JM, Le Mogne T, Boehm M, Grossiord C. Tribochemistry in the analytical UHV tribometer. Tribology International 1999;32:617-26.
[36] Buckley DH. Friction, wear, and lubrication in vacuum; NASA SP-277. Washington, D.C.: Scientific and Technical Information Office, National Aeronautics and Space Administration; 1971.
[37] Yaqoob MA, M.B. R, Schipper DJ. Design of a vacuum based test rig for measuring micro adhesion and friction force. High Performance Structures and Materials 2012;VI:261-74.
[38] Kosinskiy M, Ahmed SI-U, Liu Y, Schaefer JA. A compact reciprocating vacuum microtribometer. Tribology International 2012;56:81-8.
[39] Scherge M, Schaefer JA. Microtribological investigations of stick/slip phenomena using a novel oscillatory friction and adhesion tester. Tribology Letters 1998;4:37-42.
[40] Scherge M, Gorb S. Biological micro- and nanotribology: nature's solutions. Berlin: Springer; 2001.
[41] Mollenhauer O, Scherge M, Karguth A. Device for examining friction conditions. Application number Priority date:
[42] Lacey PI, Naegeli DW. Development of a high-vacuum wear test apparatus mounted in a scanning electron microscope. Tribotest 1999;6:115-24.
[43] Yarosh VM, Moisheev AA, Bronovets MA. Investigation of hard lubricant coatings in space in orbit around the moon. Tribotest 2002;8:301-12.
[44] Garc de Blas FJÍ, Román A, de Miguel C, Longo F, Muelas R, Agüero A. Vacuum tribological behaviour of self-lubricating quasicrystalline composite coatings. Tribotest 2004;11:103-11.
[45] Colas G, Saulot A, Godeau C, Michel Y, Berthier Y. Decrypting third body flows to solve dry lubrication issue – MoS2 case study under ultrahigh vacuum. Wear 2013;305:192-204.
[46] Nevshupa RA, Scherge M, Ahmed SU. Transitional microfriction behavior of silicon induced by spontaneous water adsorption. Surface Science 2002;517:17-28.
[47] Deulin EA, Mikhailov VP, Panfilov YV, Nevshupa RA. Mechanics and Physics of Precise Vacuum Mechanisms. Dordrecht: Springer; 2010.

[48] Herskovits J, Mappa P, Goulart E, Mota Soares CM. Mathematical programming models and algorithms for engineering design optimization. Computer Methods in Applied Mechanics and Engineering 2005;194:3244-68.
[49] Nevchoupa RA, De Segovia JL, Deulin EA. An UHV system to study gassing and outgassing of metals under friction. Vacuum 1999;52:73-81.
[50] Rusanov A, Fontaine J, Martin J-M, Le Mogne T, Nevshupa RA. Gas desorption during friction of amorphous carbon films. Journal of Physics: Conference Series 2008;100:082050.
[51] Nevshupa RA, Roman E, de Segovia JL. Origin of hydrogen desorption during friction of stainless steel by alumina in ultrahigh vacuum. Journal of Vacuum Science & Technology A 2008;26:1218-23.
[52] Rusanov A, Nevshupa R, Fontaine J, Martin J-M, Le Mogne T, Elinson V, et al. Probing the tribochemical degradation of hydrogenated amorphous carbon using mechanically stimulated gas emission spectroscopy. Carbon 2015;81:788-99.
[53] Nevshupa R, Conte M, Delgado A, Van Rijn CPD. Sample-support element for ultra-high vacuum. Application number US201013643581 20100429. Priority date:
[54] Liu H, Bhushan B. Adhesion and friction studies of microelectromechanical systems/nanoelectromechanical systems materials using a novel microtriboapparatus. Journal of Vacuum Science & Technology A 2003;21:1528-38.
[55] Nevshupa R, Conte M, Delgado A, Igartua A, Egaña F, Aranzabe A. Dispositivo de medida de fuerzas. Application number Priority date:
[56] Nevshupa R, Conte M, Van Rijn C. Measurement uncertainty of a fibre-optic displacement sensor. Measurement Science and Technology 2013;24.
[57] Deouline EA, Mikhailov VP, Eliseev ON, Sytchev VV. Parameters of loop-controlled magnetic rheology drive for segmented large mirror. 2000. p. 303-10.

Research highlights

- Correct design of an UHV tribosystem implies optimal fulfilment of conflicting requirements for seven subsystems
- The design principles were applied for development of two UHV tribometers coupled with tribophysical and tribochemical characterization techniques
- Practical lessons learnt from the development of vacuum tribosystems are discussed